*Exploration Geophysics (2005) **36**, 7–17*
Butsuri-Tansa (Vol. 58, No.1)
Mulli-Tamsa (Vol. 8, No.1)

Statics corrections for shallow seismic refraction data

Derecke Palmer[1] **Ramin Nikrouz**[1] **Andrew Spyrou**[2]

Key Words: seismic, refraction, near-surface, irregularities, GRM, artefacts

ABSTRACT

The determination of seismic velocities in refractors for near-surface seismic refraction investigations is an ill-posed problem. Small variations in the computed time parameters can result in quite large lateral variations in the derived velocities, which are often artefacts of the inversion algorithms. Such artefacts are usually not recognized or corrected with forward modelling. Therefore, if *detailed* refractor models are sought with model-based inversion, then *detailed* starting models are required.

The usual source of artefacts in seismic velocities is irregular refractors. Under most circumstances, the variable migration of the generalized reciprocal method (GRM) is able to accommodate irregular interfaces and generate detailed starting models of the refractor. However, where the very-near-surface environment of the Earth is also irregular, the efficacy of the GRM is reduced, and weathering corrections can be necessary.

Standard methods for correcting for surface irregularities are usually not practical where the very-near-surface irregularities are of limited lateral extent. In such circumstances, the GRM smoothing statics method (SSM) is a simple and robust approach, which can facilitate more-accurate estimates of refractor velocities.

The GRM SSM generates a smoothing "statics" correction by subtracting an average of the time-depths computed with a range of XY values from the time-depths computed with a zero XY value (where the XY value is the separation between the receivers used to compute the time-depth). The time-depths to the deeper target refractors do not vary greatly with varying XY values, and therefore an average is much the same as the optimum value. However, the time-depths for the very-near-surface irregularities migrate laterally with increasing XY values and they are substantially reduced with the averaging process. As a result, the time-depth profile averaged over a range of XY values is effectively corrected for the near-surface irregularities. In addition, the time-depths computed with a zero XY value are the sum of both the near-surface effects and the time-depths to the target refractor. Therefore, their subtraction generates an approximate "statics" correction, which in turn, is subtracted from the traveltimes.

The GRM SSM is essentially a smoothing procedure, rather than a deterministic weathering correction approach, and it is most effective with near-surface irregularities of quite limited lateral extent. Model and case studies demonstrate that the GRM SSM substantially improves the reliability in determining detailed seismic velocities in irregular refractors.

GENERATING DETAILED REFRACTOR MODELS FOR INVERSION

Current model-based methods for the inversion of shallow seismic refraction data consist of generating a starting model with a standard algorithm and then perturbing this initial model until the traveltimes, computed with a forward modelling program, are sufficiently consistent with the field data. Model-based inversion can include tomographic methods (Lanz et al., 1998; Stefani, 1995; Zhang and Toksoz, 1998; Zhu et al., 1992), for which the entire process is automated, as well as the more time-consuming interactive manual methods (Whiteley, 2004).

While most approaches to model-based inversion can produce a result which is consistent with the original field data, it is not uncommon for there to be significant differences between the final results with different approaches. For example, Palmer (2003) compares the results obtained with a tomographic method in which two starting models are generated automatically with the one-dimensional (1D) tau-p algorithm, and manually with the two-dimensional (2D) algorithms of the generalized reciprocal method (GRM) (Palmer, 1980, 1981, 1986). Although both starting models are refined with the eikonal wave equation (Schuster and Quintus-Bosz, 1993), the final results are quite different in both the depths to the main refractor and in the lateral positioning of a low-velocity shear zone.

The differences in depths can be largely attributed to the use of linear velocity gradients with the 1D tau-p method, whereas constant overburden velocities were used with the GRM. Although linear velocity functions are employed in most tomographic approaches, there is very little petrophysical evidence to support the parameterization of the near-surface layers in this manner. In general, most velocity gradients in the Earth are relatively gentle, and as a result, the penetration of ray paths is rarely more than 30% of the layer thickness. Because each layer is incompletely sampled, virtually any standard velocity function can be fitted to traveltime data with acceptable accuracy (Hagedoorn, 1955; Palmer, 1986, p.169–175; 1992). Furthermore, hyperbolic velocity functions can be readily fitted to traveltime graphs consisting of linear segments (Slichter, 1932; Healy, 1963; Berry, 1971; Aki and Richards, 2002, p.422). Such velocity functions can result in the computed depths being more than 70% greater than would be the case if constant seismic velocities were fitted to the same traveltime graphs. The issues related to the parameterization of the overburden layers will not be considered further in this study.

The differences in the lateral positioning of the zone with the low seismic velocity in the refractor are related primarily to the algorithm used to generate the starting model, and it is the subject of this paper. This study addresses this issue in two parts.

The first part seeks to show that the detailed lateral resolution of seismic velocities in the refractor is an ill-posed problem, that

[1] *School of Biological, Earth and Environmental Sciences*
University of New South Wales
Sydney NSW 2052, Australia
Email: d.palmer@unsw.edu.au

[2] *formerly School of Biological, Earth and Environmental Sciences*
University of New South Wales, Sydney NSW 2052
now Fugro Ground Geophysics Pty Ltd

Manuscript received November 3, 2004.
Revised manuscript received December 1, 2004.

is, small variations in the computed time parameters can result in large variations in the derived seismic velocities. This problem can be especially acute with seismic refraction surveys carried out for near-surface targets, because the traveltime differences between receivers, which are often separated by as little as 2.5 m, can be much the same as the errors in measuring those traveltimes. The major conclusion of this part of the study is that simplified algorithms for computing seismic velocities in the refractor can generate artefacts, which are not necessarily recognized nor corrected with most approaches to model-based inversion. Therefore, if detailed lateral variations in refractor velocities are the objective, then algorithms that can generate detailed starting models are required, so that the inversion process can converge to a most likely model.

Frequently, irregular refracting interfaces are the major source of artefacts in the initial refractor model. Model and case studies (Palmer, 1980; 1981; 1986; 1991) demonstrate that the GRM is usually able to determine useful refractor parameters with irregular interfaces.

However, the effectiveness of the GRM algorithms can often be reduced where there are irregularities in the very-near-surface layers (Palmer, 1980, p.22–24). In many cases, these irregularities can be defined and corrected with standard methods (Dobrin, 1976, p. 334–336; Palmer, 1986, p.152–155), using traveltimes obtained with intermediate shot-to-receiver spacings. Unfortunately, this approach is not efficacious where the near-surface irregularities extend over very limited lateral distances, because they cannot be mapped directly with reversed traveltime data. As a result, neither their seismic velocities nor their thickness can be computed with the standard approach. Furthermore, the methods normally employed for the acquisition of common-midpoint reflection data, such as the use of extended receiver arrays and extended surface source arrays, usually do not generate traveltime data of sufficient quality from the surface layers. Accordingly, another method is required to correct for the very-near-surface irregularities.

The second and major part of this study presents a new method for accommodating the very-near-surface irregularities or "statics", in order to generate more-accurate starting models of the refractor velocities. It is based on the GRM, it uses traveltimes from a deeper refractor, and it is termed the GRM smoothing statics method (GRM SSM).

The significance of the near-surface irregularities has been highlighted with a recent three-dimensional shallow refraction survey carried over a major shear zone associated with dryland salinity at Spicers Creek, near Dubbo in southeastern Australia (Nikrouz, Spyrou, and Palmer, in prep). While the GRM velocity analysis algorithm was able to generate useful starting models for inversion for each line, the consistency between adjacent parallel lines, which were separated by 10 m, was not always obvious. As discussed within this study, relatively small variations in the refractor velocity analysis algorithm resulted in significant changes in both the computed values of the seismic velocities and their lateral extent. The use of the GRM SSM described here was a major factor in achieving improved consistency between adjacent lines, and in turn, with improving the spatial resolution of the shallow seismic refraction results.

However, even routine 2D refraction investigations can benefit significantly from the application of the GRM SSM. The case study describes a single seismic refraction profile recorded across a narrow massive sulphide orebody at Mt Bulga in southeastern Australia. This survey was carried out to test whether a density model could be derived from the head wave amplitudes. As it was anticipated that there would be an unambiguous increase in density

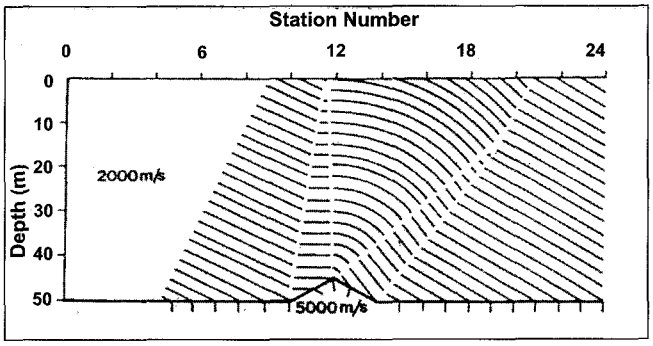

Fig. 1. Wavefront construction for a model with a small irregularity in an otherwise uniform refractor. The increment in wavefronts is 1 ms. All of the arrivals, which originate from the irregularity, are diffractions. The station spacing is 5 m.

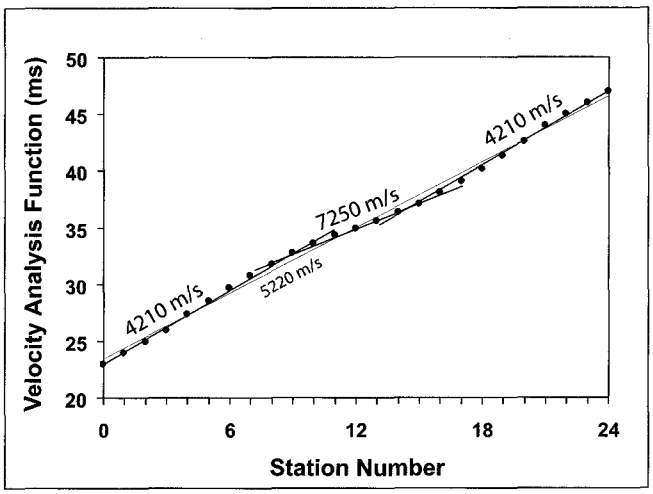

Fig. 2. Velocity analysis function of the conventional reciprocal method computed for the model in Figure 1. Two quite different velocity models can be fitted to the computed points to an accuracy of better than one millisecond.

associated with the mineralization, any variations in head wave amplitudes would provide a first step in assessing the feasibility of the concept.

The determination of in-situ density models with shallow seismic refraction methods could prove useful for the detailed inversion of gravity data, such as that obtained with high-resolution airborne gravity gradiometers. Furthermore, the determination of densities together with seismic velocities could facilitate the computation of bulk in-situ elastic constants for geotechnical studies.

The theoretical basis for the derivation of in-situ densities from head wave amplitudes is relatively straightforward. Palmer (2001a) demonstrates that the product of the forward and reverse head wave amplitudes compensates for geometric spreading and that the result is proportional to the head coefficient. (The head coefficient is analogous to the transmission coefficient of the Zoeppritz equations, and describes the head wave amplitude in terms of the petrophysical properties in the two media.) Furthermore, Palmer (2001b) shows that the head coefficient is proportional to the ratio of the specific acoustic impedances, which is the product of the seismic velocities and densities, in the overburden and the refractor. Therefore, if the detailed lateral variations in the refractor velocities can be resolved with the traveltime data, then the possibility exists for the derivation of a model of the lateral variations in the bulk in-situ densities from the amplitude data.

The irregular near-surface conditions at the Mt Bulga site generated numerous traveltime anomalies, which were a limiting factor in unambiguously determining the seismic velocities in the main refractor. As a result, the uncertainties in the seismic velocities limited the accuracies in deriving estimates for the in-situ densities from the head wave amplitudes.

NON-UNIQUENESS IN DETERMINING DETAILED REFRACTOR VELOCITIES

That the determination of the seismic velocities in the refractor is an ill-posed problem can be readily demonstrated with the simple model in Figure 1. It consists of a small irregularity in an otherwise uniform refractor. All of the first arrival traveltimes associated with the irregularity are diffractions. The station interval is 5 m.

The inversion algorithms of the conventional reciprocal method (Hagiwara and Omote, 1939; Hagedoorn, 1959; Hawkins, 1961) provide one of the simplest approaches to deriving a starting model (Whiteley, 2004). The first task is to determine the seismic velocity in the refractor through the differencing of the forward and reverse traveltimes with equation (1), namely

$$t_V = \left(t_{forward} - t_{reverse} + t_{reciprocal}\right)/2 \quad . \tag{1}$$

The values computed with equation (1) are shown in Figure 2. The seismic velocity in the refractor V_n, is the reciprocal of the gradient, as in equation (2):

$$\frac{d\,t_V}{dx} = 1/V_n \quad . \tag{2}$$

Although the application of equation (1) is quite straightforward, the determination of the refractor velocity(s) with equation (2) is subject to considerable personal judgment. Figure 2 shows that the computed values are strongly linearly correlated, and that a single line, representative of a seismic velocity of 5220 m/s can be fitted with an accuracy of better than one millisecond.

However, the vast majority of geoscientists would fit three segments with seismic velocities of 4210 m/s, 7250 m/s and 4210 m/s, as is shown in Figure 2, simply because the much improved visual fit results in residuals which are essentially zero. The change in seismic velocities from 4210 m/s to 7250 m/s, representing an increase of 72%, is very large and for that reason alone, it would normally be accepted as a genuine lateral variation. Furthermore, such a large increase in seismic velocities would have important implications in most shallow seismic investigations. Nevertheless, the lateral variations in the refractor velocities are artefacts of the inversion algorithm.

This example demonstrates some of the deficiencies with the conventional reciprocal method and most importantly, the fact that the determination of refractor velocities is an ill-posed problem: small variations in the refractor velocity analysis function can result in major changes in the computed seismic velocities. In Figure 2, variations of approximately one millisecond in the velocity analysis function can lead to the inference of lateral variations, which differ from the true refractor velocity of 5000 m/s by 16% and 45%. Furthermore, it is not possible to infer whether even large lateral variations in the refractor velocities are genuine, or whether they are artefacts of the velocity analysis algorithm of the conventional reciprocal method, because there are no accepted objective criteria for distinguishing either.

Figure 3 shows the time-depths generated using equation (3) with XY values of zero, which is the conventional reciprocal method, and 40 m, which is approximately the optimum value. (The time-depth is mathematically equivalent to the half-intercept time or the mean delay time, and it is a measure of the depth to the refractor in units of time.) The XY distance, which is the separation between the reverse and forward traveltimes, seeks to accommodate the offset distance, which is the horizontal separation between the point of refraction on the interface and the point of measurement on the surface.

$$t_G = \left(t_{forward} + t_{reverse} - t_{reciprocal} - XY/V_n\right)/2 \tag{3}$$

The time-depths computed with a zero XY value show two regions approximately 45 m wide on either side of station 12, for which the values are smaller due to the irregularity in the refractor. Furthermore, the minimum time-depths occur at stations 8 and 16 with a zero XY value rather than at station 12, which is at the apex of the irregularity in the refractor.

Figure 4 shows the depth section computed with a zero XY value, that is, with the conventional reciprocal method. The depths are computed with equation (4),

$$\begin{aligned} Z_G &= t_G \frac{V_n V_1}{\sqrt{V_n^2 - V_1^2}} \quad , \\ &= t_G\, DCF \end{aligned} \tag{4}$$

where DCF is the depth conversion factor and

$$DCF = \frac{V_n V_1}{\sqrt{V_n^2 - V_1^2}} = \frac{V_1}{\cos i_{1n}}$$

and (5)

$$\sin i_{1n} = \frac{V_1}{V_n}$$

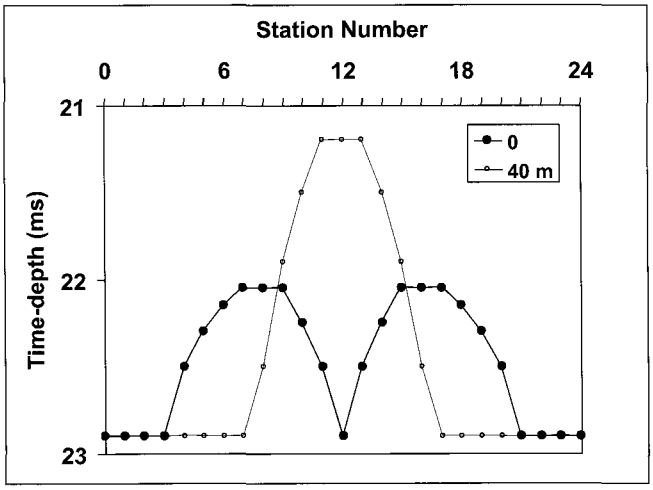

Figure 3. Time-depths computed for the model in Figure 1. The time-depths computed with a zero XY value show two regions approximately 45 m wide on either side of station 12, for which the values are smaller due to the irregularity in the refractor. Furthermore, the minimum time-depths occur at stations 8 and 16 with a zero XY value rather than at station 12, which is at the apex of the irregularity in the refractor in Figure 1.

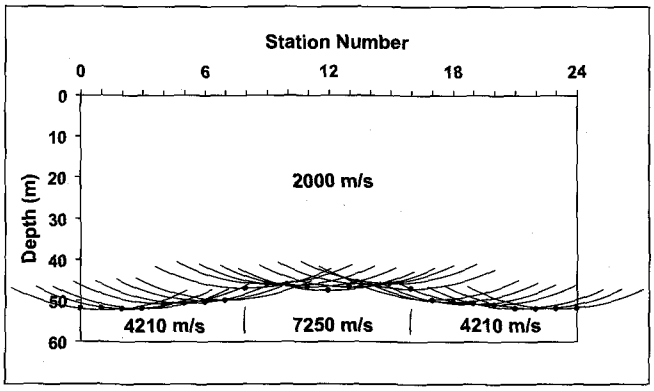

Fig. 4. Starting model generated with the conventional reciprocal method. The reduction in depths centred on station 12 corresponds with a large increase in the seismic velocities, and therefore, it is geologically reasonable.

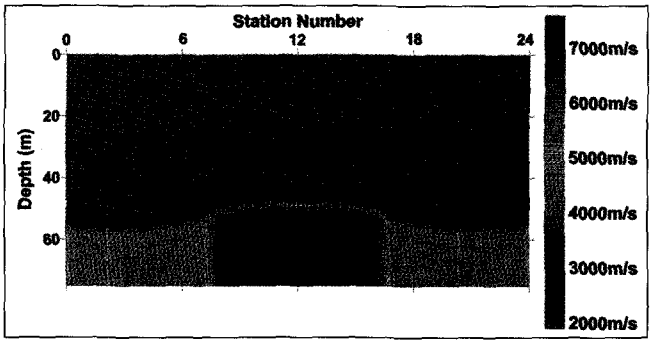

Fig. 5. Final model derived from the starting model in Figure 4 generated with the conventional reciprocal method, using refraction tomography and the eikonal wave equation.

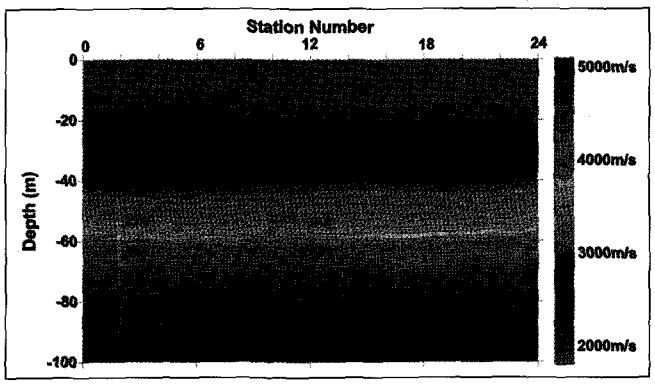

Fig. 6. Final model derived with refraction tomography and the eikonal wave equation, using a starting model generated automatically by the computer program with the tau-p algorithm.

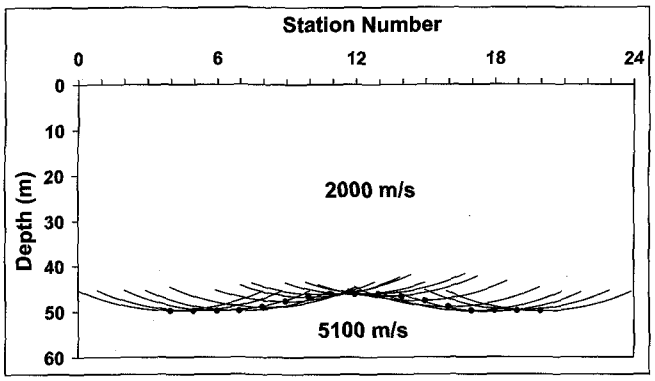

Fig. 7. Starting model generated with the algorithms of the GRM.

Figure 4 demonstrates that the conventional reciprocal method has done a barely adequate job in reproducing the model. There are errors in depths, related both to refractor velocity "pull-ups" and "pull-downs" and to the unfocussed time-depths on either side of station 12. Although the decrease in depths near station 12 can still be recognized, the apex is now reproduced as a 20 m wide region. Furthermore, its correlation with the increase in refractor velocities gives it geological verisimilitude, and therefore under most circumstances the depth cross-section would be considered acceptable.

Forward modelling of Figure 5, which is a refraction tomogram using a starting model derived from Figure 4, with the eikonal wave equation (Schuster and Quintus-Bosz, 1993), produces a mean unsigned error of 0.894 ms, and a relative misfit function of 0.554 ms (Schuster and Quintus-Bosz, 1993, p. 1315). Therefore, when the conventional reciprocal method is applied objectively without editing for which there are no clearly defined criteria, the depth cross sections shown in Figures 4 and 5 would be the most likely result. Clearly, forward modelling neither recognizes nor corrects the artefacts in the refractor velocities.

Figure 6 shows the depth cross-section derived from 1D inversion using the tau-p algorithm and linear velocity gradients. Forward modelling with the eikonal wave equation (Schuster and Quintus-Bosz, 1993), produces a mean unsigned error of 0.388 ms, and a relative misfit function of 0.230 ms (Schuster and Quintus-Bosz, 1993, p. 1315). The depths to the 5000 m/s contour are approximately 85 m, which is an error of 70%, while the refractor irregularity at station 12 occurs over approximately 60 m between stations 6 and 18.

A GRM analysis of the model in Figure 2 (Palmer, 1986, p.111–117) produces the result shown in Figure 7. The computed refractor velocity is 5100 m/s, for an error of 2%. Figure 7 demonstrates that the GRM both accommodates diffractions associated with the refractor irregularity and only images those parts of the refractor from which first arrival energy is received. As a corollary, this study shows that an important consequence of the occurrence of diffractions with irregular refractors is that they result in an incomplete definition of the interface (Palmer, 1980, p.29; 1986, p.117; Sjogren, 1984, p.84–95). Only those parts of the interface are defined where the radius of curvature is greater than the layer thickness, and as a result, a smoothed version of the refractor is obtained. Therefore, the use of ray-tracing routines which rigorously apply Snell's law, such as the modified Ackermann version (Ackermann et al., 1986) employed by Leung (1997, 2003) and (Whiteley, 2004), can be inappropriate with irregular interfaces, because the true position and in turn, the true dips of the interface are not known. Forward modelling routines, which can accommodate diffractions, such as wavefront reconstruction (Schuster and Quintus-Bosz, 1993) can be a more useful alternative approach. Forward modelling of Figure 7 with the eikonal wave equation produces the depth cross section in Figure 8, with a mean unsigned error of 0.769 ms, and a relative misfit function of 0.420 ms (Schuster and Quintus-Bosz, 1993, p. 1315).

These results demonstrate that it is possible to obtain satisfactory agreement with the traveltime data for a range of starting models. Therefore, while agreement with the traveltime data can demonstrate that any particular model is acceptable, it does not demonstrate that the model is either "correct" or unique.

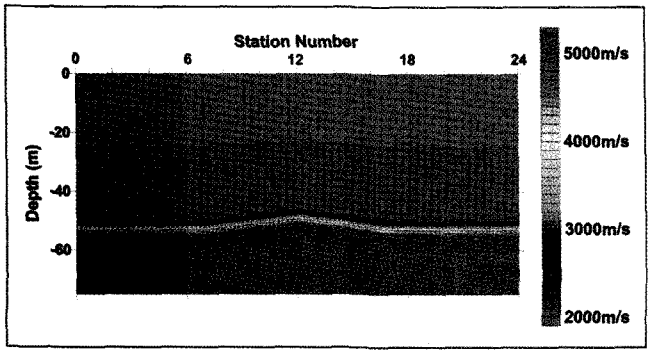

Fig. 8. Final model derived from the starting model in Figure 7 generated with the GRM, using refraction tomography and the eikonal wave equation.

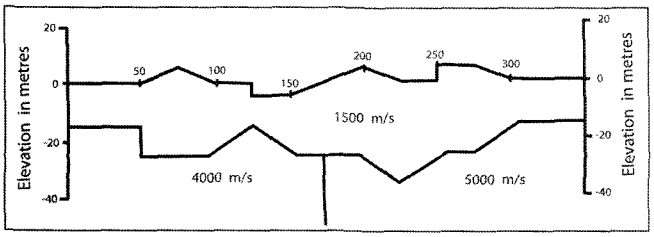

Fig. 9. Model showing an irregular refractor with a lateral change in the seismic velocity and an irregular surface topography. The model extends over an horizontal distance of 350 m.

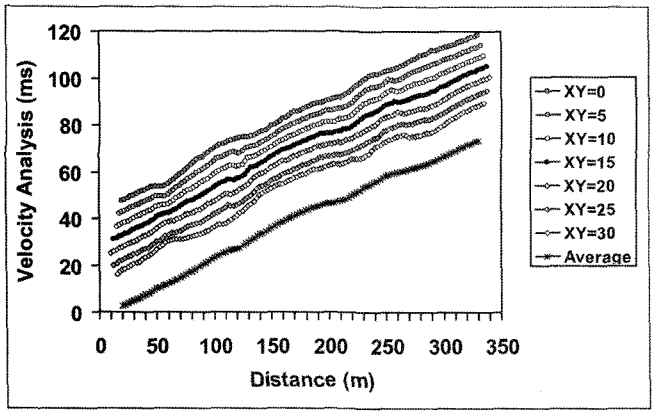

Fig. 10. The refractor velocity analysis function for a range of XY values from zero to 30 m. The graphs for individual XY values have been separated for clarity by adding a constant value. Individual graphs are irregular because both the refractor and the topography are irregular. The average of these graphs is smoother, but still sufficiently irregular to generate artefacts.

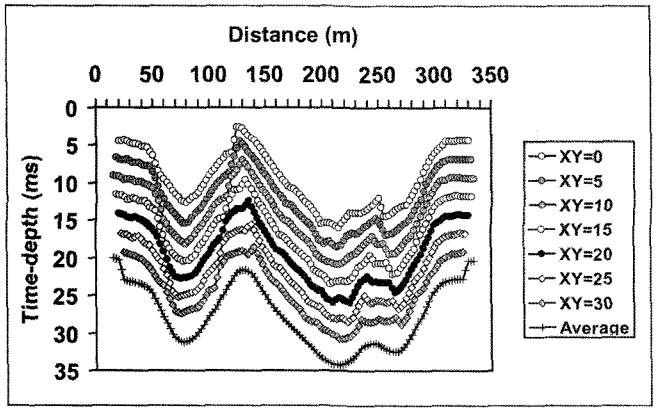

Fig. 11. Time-depths generated with XY values from zero to 30 m. The time-depths reflect the irregularities in both the surface topography and the refractor. The abrupt changes in the surface topography at 130 m and 250 m generate anomalies, which propagate laterally through the time-depth profiles with increasing XY values.

Non-uniqueness has yet to be adequately addressed in the inversion of shallow seismic refraction data. Perhaps one of the more useful statements of non-uniqueness, which alludes to the importance of the algorithm used to generate the starting model, is the following paragraph from Oldenburg (1984, p.666).

"For many investigators the primary goal of inverse theory is to generate a model which reproduces the observations. The structure observed on m(z) (*Oldenburg's model parameters*) may be interpreted directly, or m(z) may be the input to further modelling. A fundamental problem, however, is that m(z) is a function on the Hilbert space H[0,a] (*Oldenburg defines the model over the interval [0,a]*), and consequently there will be infinitely many functions in that space which can reproduce a finite number of observations. This non-uniqueness becomes more severe when the data are inaccurate and when models which do not fit the data precisely are considered acceptable. Loosely speaking, a particular algorithm generates a particular type of model. This, coupled with the non-uniqueness of the solution, suggests that a good approach to the construction problem is to design a number of different algorithms which can reproduce a variety of acceptable models. Not only will such an approach provide valuable insight regarding non-uniqueness but some models which are judged to be more likely from a physical basis (or personal prejudice) may be selected as best "guesses" to the true model."

Not only is Oldenburg stating that non-uniqueness is an essential aspect of model-based inversion (see also Treitel and Lines, 1988) but he is also stating that the generation of a multiplicity of models is to be encouraged. The GRM can generate such a multiplicity of models, simply by employing different XY values. Each of these models agrees with the traveltime data (Palmer, 1980, p.50; Palmer, 1986, p. 156–162). Furthermore, the minimum variance criterion of the GRM facilitates the recognition of a most likely starting model.

"STATICS" CORRECTIONS FOR SHALLOW REFRACTION DATA – MODEL STUDY

The new method for correcting for near-surface irregularities, the GRM SSM, will be demonstrated with the model shown in Figure 9, which is taken from Palmer (1980, Fig. 14). This model, which is rather extreme with both an irregular refractor and irregular topography, has a lateral change in the seismic velocity in the refractor.

The first step is to generate the refractor velocity analysis function for a range of XY values from less than to greater than the optimum XY value with equation (1). The results are shown in Figure 10. The graphs for individual XY values have been separated for clarity by adding a constant value, which is readily achieved by systematically increasing the reciprocal time for each XY value.

The graphs are irregular because both the refractor and the topography are irregular. Palmer (1980, Fig. 6) shows that, for an irregular refractor and flat topography, the velocity analysis graphs are essentially symmetrical about that computed with a 20 m XY value, while the graphs are symmetrical about the set computed with a zero XY value for a flat refractor and irregular topography (Palmer, 1980, Fig. 11). The graphs in Figure 10 exhibit no clear symmetry about any particular XY value because of these two separate competing effects. The aim of the GRM SSM is to minimize the effects of the near-surface irregularities, so that the symmetry of the velocity analysis graphs about an optimum value, which is representative of the target refractor, can be more easily recognized.

An average for XY values from zero to 30 m has been computed, and is shown in Figure 10. Although this average is not as irregular as the graphs computed with individual XY values, there are still a number of changes in slope to which the detailed application of equation (2) would result in the generation of artefacts in the refractor velocities.

The second step is to compute time-depths with equation (3). The results are shown in Figure 11. The term XY / V_n is approximated with the difference in the averaged velocity analysis function over the same interval, i.e.,

XY / V_n = averaged velocity analysis function at Y
- averaged velocity analysis function at X . (6)

Where the surface topography is flat, there are usually relatively small differences in the time-depths computed with different XY values for an irregular refractor (Palmer, 1980, Fig. 7). (As an aside, the differences are much the same as those differences obtained with the refractor velocity analysis function (Palmer, 1980, Fig. 6). While these differences can result in the computation of a wide range of seismic velocities in the refractor with equation (2), they are not as critical with the time-depths.)

However, the time-depth anomalies associated with the irregular surface topography propagate laterally throughout the time-depths as the XY value is varied (Palmer, 1986, p.107–111). For example, suppose that there is a single near-surface irregularity, which results in coincident anomalies on the forward and reverse traveltime graphs. For a zero XY value, the time-depths will exhibit an anomaly equal to that in the traveltime graphs. As the XY value is increased, the coincidence between the forward and reverse traveltime graphs is lost, and two time-depth anomalies, half the traveltime anomaly and separated by the XY distance, are generated. The pattern of the lateral migration of the surface anomalies can be recognized with the escarpment features at 130 m and 250 m in Figure 11, and with the anomaly centred on station 56 in Figure 18.

The third step is the generation of the "statics" corrections by subtracting the time-depths averaged over a range of XY values from the time-depths computed with a zero XY value. When an average of the time-depths is computed, the loss in resolution of the refracting interface is relatively minor. However, the anomalies due to the near-surface irregularities are greatly reduced through the averaging process, because they systematically propagate laterally with increasing XY values. Therefore, to a reasonable first approximation, the averaged time-depth profile represents the values for the target refractor, which has been partially corrected for the near-surface irregularities. Furthermore, the time-depth profile computed with a zero XY value represents the sum of the time-depths for both the near-surface irregularities and the target refractor. Therefore, the difference between the time-depths computed with a zero XY value and the time-depths averaged over a range of XY values generates the smoothed anomalies due to the near-surface irregularities. These anomalies are then subtracted from the traveltime data, and the computation of the velocity analysis graphs and the time-depths is repeated.

The corrections computed with this procedure show very little correlation with the surface topography. Accordingly, they represent more of a smoothing process, rather than a deterministic weathering correction procedure (Dobrin, 1976, p. 334–336; Palmer, 1986, p.152–155). This is also supported by the fact that, for the maximum elevation changes of ±5 m in Figure 9, the maximum statics would be approximately 3 ms (5 m / 1500 m/s), whereas the maximum correction computed with the GRM SSM is 0.97 ms, the average is 0.01 ms and the standard deviation is 0.40 ms.

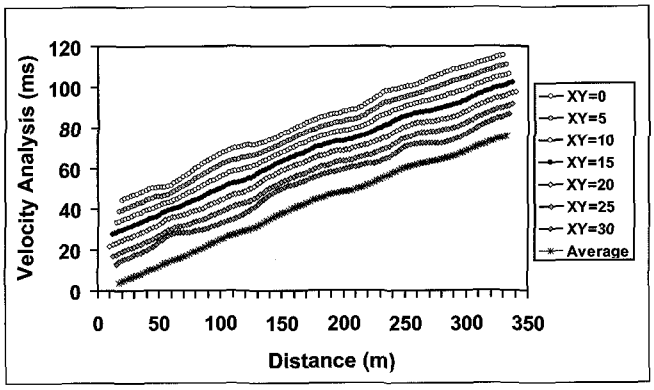

Fig. 12. GRM refractor velocity analysis graphs, which have been corrected with the GRM SSM. There is a clear improvement in the symmetry of the refractor velocity analysis graphs about the graph for 15 m XY value, compared with Figure 10.

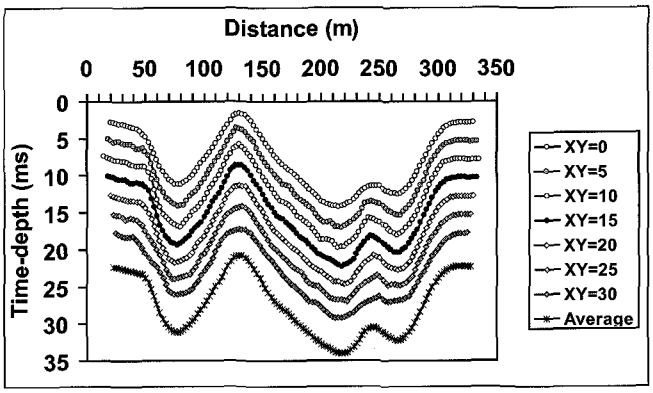

Fig. 13. GRM time-depth graphs, which have been corrected with the GRM SSM. The time-depths exhibit considerably less variation, compared with Figure 11.

Figures 12 and 13 show the refractor velocity analysis and the time-depth functions after one application of the GRM SSM. There is a clear improvement in the symmetry of the refractor velocity analysis graphs about the graph for 15 m XY value. In addition, the time-depths exhibit considerably less variation.

While the GRM SSM has significantly reduced the artefacts related to the topographic irregularities, the compensation is not complete. It has been found that several iterations of the GRM SSM can produce systematic improvements in the symmetry of velocity analysis graphs about an optimum, and that there is a systematic reduction in refractor velocity artefacts as a result.

Furthermore and contrary to normal expectations, the method appears to work much better with normal field data, than with model data, as will be demonstrated in the case study to follow. In such cases, one application of the GRM SSM has usually proven to be sufficient.

"STATICS" CORRECTIONS FOR SHALLOW REFRACTION DATA – CASE STUDY

The case study consists of a single seismic refraction profile recorded across a narrow massive sulphide orebody at Mt Bulga in southeastern Australia. The case study is complex as there are lateral changes in the seismic velocities in both the refractor and the weathered layer. In addition, the mineralization is narrow, commonly about 5 m, and as a result, the lateral limits of resolution of the seismic refraction method were expected to be an issue.

Nine shots, each consisting of small explosive charges in shallow hand-augured shot holes, and nominally 30 m apart, were

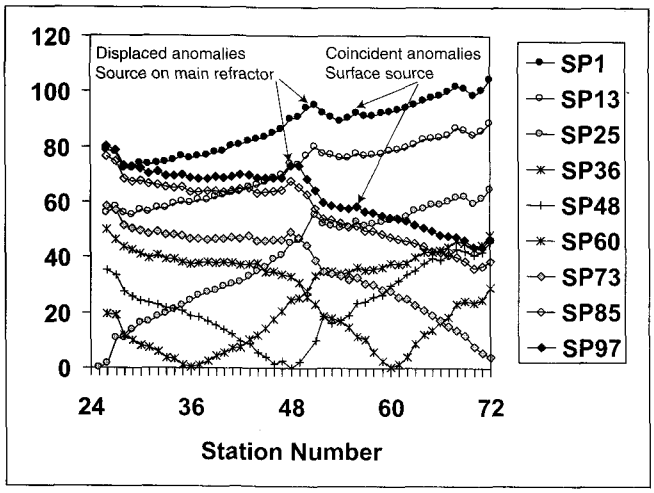

Fig. 14. Traveltime graphs recorded across a narrow massive sulphide orebody. Traveltime anomalies are caused by both near-surface irregularities and significant changes in the depth to and the seismic velocity within the main refractor.

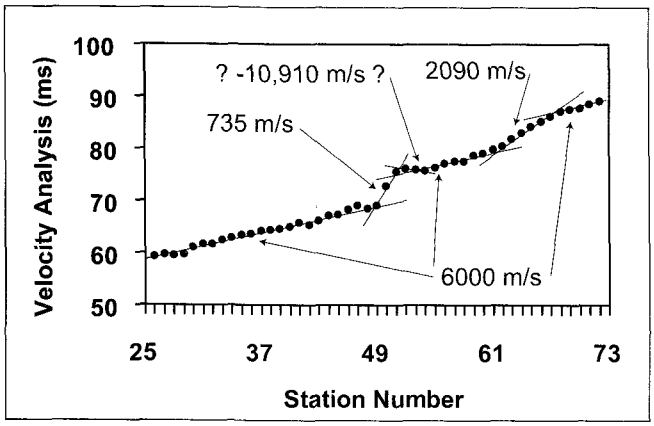

Fig. 15. The refractor velocity analysis function of the conventional reciprocal method. The abnormally low seismic velocity of 735 m/s and a physically unrealistic velocity of -10 910 m/s occur near station 49, which is the approximate location of the sulphide mineralization.

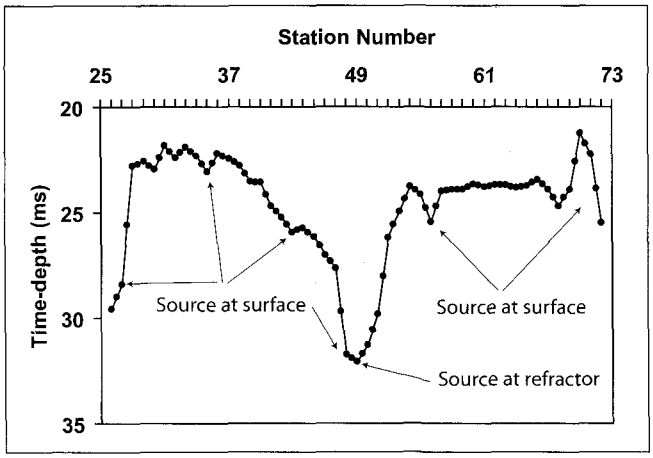

Fig. 16. Time-depth profile computed with the conventional reciprocal method. The large increase at station 49 indicates that the refractor velocities are likely to be artefacts

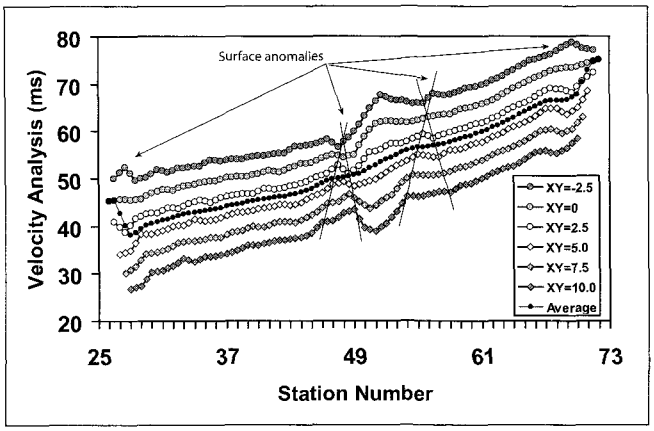

Fig. 17. GRM refractor velocity analysis function for XY values from -2.5 m to 10 m. The average has minimized the artefacts caused by the increase in depths to the refractor around station 49. However, the probable occurrence of a near-surface irregularity at 48 introduces some uncertainty in the detailed velocity determinations.

recorded with a 48 trace seismic system using single geophones, which were 2.5 m apart. The centre of the seismic line at station 49 was located on the crest of a small ridge, which also marks the approximate location of the sulphide orebody. The rocks on either side of the mineralization are Silurian meta-sediments. Between stations 25 and 43, these sediments crop out, and there were some difficulties both in auguring the shot holes to a satisfactory depth and in planting the geophones. Nevertheless, the geophone spikes were still inserted into the ground, although sometimes not to the full 75 mm length, and the geophones can still be considered to be well coupled. Between stations 43 and 73, there is no outcrop, and the production of the shot holes was much easier, as was the planting of the geophones. These surface conditions generated near-surface irregularities, which often only occurred at single receiver locations.

The traveltime graphs in Figure 14 show that a two-layer model of the seismic velocities is generally satisfactory, and that there is a significant lateral change in the seismic velocities of the first layer. Between stations 25 and 43 where the Silurian meta-sediments sediments crop out, the seismic velocity of the first layer is 1830 m/s. Between stations 43 and 73 there is little or no outcrop, and the seismic velocities of the first layer range from 900 m/s to 1200 m/s.

At station 56, there are small, but detectable increases in both the forward and reverse traveltimes. These increases are inferred to be the result of an increase in the thickness of surface layer of soil, or possibly a reduction in the seismic velocities of the near-surface region, because there is no lateral offset between these increases in the forward and reverse traveltime graphs.

By contrast, about two receiver intervals, or 5 m, separate the increases of approximately 10 ms in the traveltimes in the forward and reverse directions on either side of station 49. This separation is in fact twice the offset distance, which is the horizontal separation between the point of critical refraction on the refractor and the point of detection of the refracted ray at the surface. These increases in the traveltimes are the result of an increase in depth to the unweathered rock, a local decrease in the seismic velocities of partially compacted fill associated with recent restoration, or a combination of both.

Figure 15 presents the refractor velocity analysis function of the conventional reciprocal method. Near station 49, which is the approximate location of the sulphide mineralization, the results suggest both an abnormally low seismic velocity of 735 m/s over a horizontal interval of 5 m, as well as a physically unrealistic velocity of -10 910 m/s. These obviously questionable velocities in the refractor correlate with an increase in the time-depths, as shown in Figure 16, and in turn, with a probable increase in depth to the main refractor. The surface anomaly at station 56 is evident as an increase of about 1 ms in the time-depth profile in Figure 16.

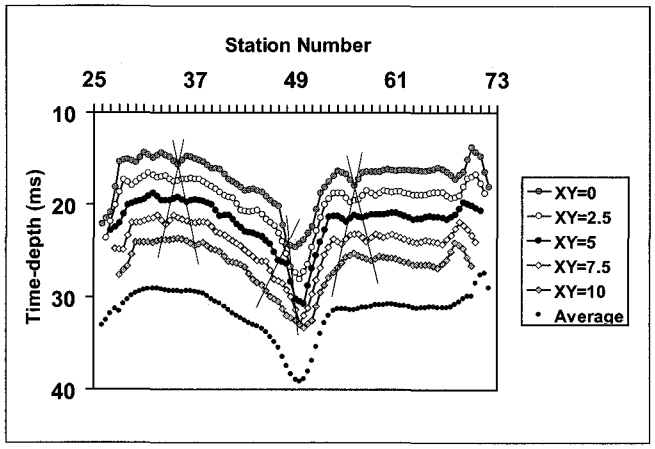

Fig. 18. The GRM time-depth profiles for XY values from zero to 10 m. The near-surface irregularities and their lateral migration with increasing XY distances are highlighted. The averaged time-depth profile is largely unaffected by the near-surface irregularities.

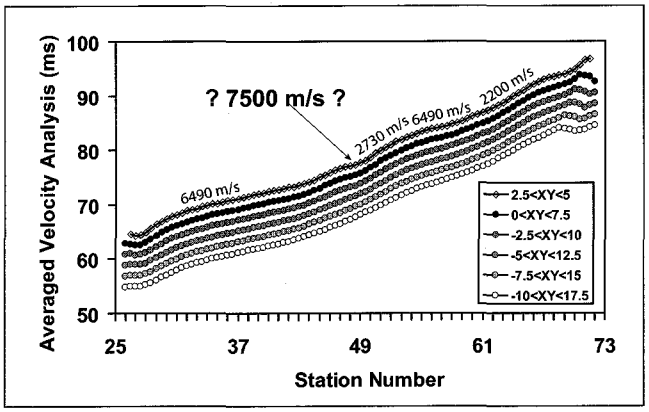

Fig. 20. The averaging of the refractor velocity graphs in Figure 19 greatly reduces the artefacts caused by refractor architecture. From Figure 19, the optimum XY value appears to be between 2.5 m and 5 m. Therefore, the range of the XY values used in the averaging process is symmetrical about these values. It is possible that the interval with the seismic velocity of 7500 m/s may exist.

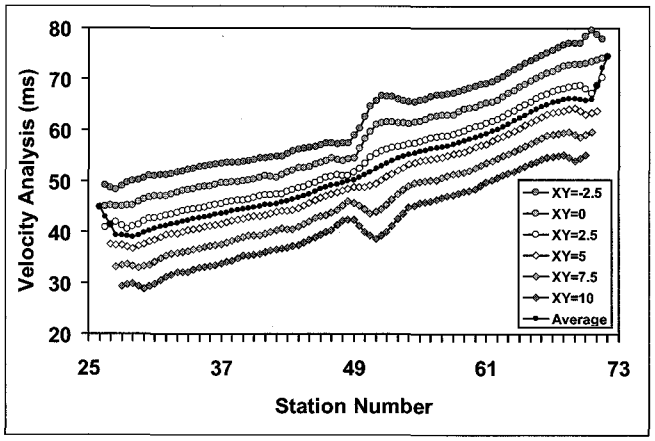

Fig. 19. GRM refractor velocity analysis graphs computed with traveltimes that have been corrected with the GRM SSM. The effective removal of the near-surface anomalies results in a clear improvement in the symmetry of the graphs about the average.

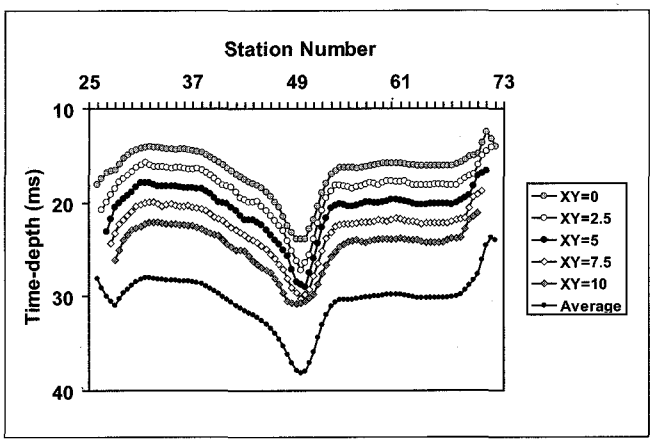

Fig. 21. GRM time-depths computed with the traveltimes corrected for the near-surface irregularities. They have been largely removed.

It is likely that the unusual seismic velocities are artefacts related to the architecture of the refractor. However, apart from verisimilitude, there is no objective criterion for determining the veracity of these velocities. Clearly, an approach such as the GRM, which can usually resolve genuine lateral changes in refractor velocities from artefacts generated by the inversion algorithm, is required. Figure 17 presents the GRM refractor velocity analysis algorithm for XY values from -2.5 m to 10 m.

While there is probably limited geophysical significance for negative XY values, the computed graphs can facilitate the definition of the symmetrical pattern about the optimum XY value, especially where the optimum is much the same value as the receiver spacing. Furthermore, these graphs can be very useful where the averaging of several sets of graphs, which are symmetrical about the optimum, are employed to reduce the effects of artefacts caused by refractor architecture.

The velocity analysis graphs exhibit the familiar symmetry about the optimum XY value, which in this case appears to be between 2.5 m and 5 m. An average of the graphs, which are symmetrical about the optimum, that is, for XY values between -2.5 m and 10 m, greatly minimizes the artefacts due to the refractor architecture.

The results in Figure 17 indicate that there is a narrow region between stations 48 and 49 where the seismic velocity in the refractor is quite high. However, this region also appears to exhibit the same signature due to a surface anomaly, as that at station 56 (see also Palmer, 1986, Figure 8–9). The coincidence of the possible near-surface irregularity, probably caused by the recent restoration of the site, with the large increase in time-depths in the refractor introduces some uncertainty in the detailed resolution of the refractor velocities.

Figure 18 shows the time-depths computed for a range of XY values from zero to 10 m, together with the average of these values. Several near-surface irregularities, such as that at station 56, can be recognized by their lateral migration through the time-depths with increasing XY distances. The average of the time-depths has removed the time anomalies associated with these near-surface irregularities, but it has still largely preserved the architecture of the refractor.

Figure 19 presents the refractor velocity analysis function computed with the traveltimes corrected with the GRM SSM. Qualitatively, the individual graphs are smoother than those in Figure 17, and the symmetry about the optimum XY, which is between 2.5 m and 5 m, is clearer. Averaging these graphs over various ranges of XY values as shown in Figure 20, indicates that there may be a narrow zone with a low seismic velocity.

Figure 21 presents the time-depth computed with same corrected traveltimes, and it can be seen that the effects of the near-surface

irregularities have been largely removed. Furthermore, the average in Figure 21 is much the same as that in Figure 18, indicating that any loss in resolution is minimal.

CONCLUSIONS

The determination of seismic velocities in the unweathered layer with shallow seismic refraction methods is often an ill-posed problem. Very small variations in the parameters used to derive the seismic velocities in the refractor can result in significant variations in the computed velocities. In many cases, where small receiver spacings are employed to define very shallow targets, such as is commonly the case with geotechnical investigations, the variations in the computed time parameters are often as large as the errors in the traveltime data.

If a low-resolution model of the refractor velocities is required, then the conventional reciprocal method is quite adequate. The major advantage of this method is that it is able to accommodate near-surface irregularities without the need to make explicit corrections (Palmer, 1986, p.60–63). However, the common temptation is to seek greater resolution than numerous model and case studies demonstrate is achievable with the method, and this frequently results in the generation of artefacts.

Generally, the artefacts in the seismic velocities in the refractor are associated with changes in depth to the refractor. The first model described in this study demonstrates that even relatively small irregularities in the architecture of the refractor can produce quite significant artefacts. The likely occurrence of artefacts in routine field surveys can often be indicated where significant lateral changes in refractor velocities are associated with changes in depth to the refractor.

Artefacts are usually neither recognized nor corrected with forward modelling, such as with ray tracing for example, because the differences in the computed time parameters for the various models are usually within acceptable limits. Furthermore, there is no objective criterion for perturbing the starting model with manual interactive approaches, and the verisimilitude criterion is usually employed.

The inability of forward modelling to recognize or correct artefacts is consistent with the fundamental non-uniqueness of all methods of model-based inversion. In general, non-uniqueness is not adequately addressed with most approaches to shallow refraction inversion. However, the reality of non-uniqueness indicates that the current contractual requirement for many geotechnical investigations of employing the conventional reciprocal method together with a ray-tracing routine, in order to prevent claims for compensation for variations in conditions, might not necessarily survive a legal challenge.

The use of the GRM to recognize and accommodate artefacts due to the architecture of the refractor has been demonstrated with numerous model and case studies. However, the efficacy of the GRM can be reduced where there are surface irregularities, commonly within the first few metres of the surface. In these circumstances, the very low seismic velocities of the dry soil layers often produce significant time anomalies, which can adversely affect the detailed resolution of any lateral variations in the seismic velocities in the refractor.

In many cases, the near-surface layers are sufficiently thick and of sufficient lateral extent to be adequately mapped with the standard methods, using traveltime data recorded with intermediate shot-to-receiver offsets. However, these methods are not applicable where the near-surface irregularities extend over only a few receiver stations at most. Under those conditions, an alternative approach is required.

The GRM SSM is a simple but robust method to compensate for near-surface irregularities, which uses the traveltimes from a deeper refractor, usually the target refractor. It is efficacious because the time-depths for an irregular refractor do not alter substantially with varying XY distances, whereas the time-depths for a near-surface irregularity propagate laterally with increasing XY values. An average of the time-depths over a range of XY values generates a profile of the refractor which is very similar to that obtained with the optimum XY value. However, the time-depths for the near-surface irregularities are reduced through the averaging process. Therefore, when the averaged time-depth profile is subtracted from that computed with a zero XY value, the result is a correction for the near-surface "statics".

The application of these "static" corrections to the traveltime data usually produces velocity analysis graphs which exhibit better symmetry about the optimum XY value, and which therefore facilitate more reliable estimations of the seismic velocities in the refractor. However, the "statics" corrections are usually less than a millisecond and therefore, they do not substantially alter the average time-depth profile of the target refractor.

The GRM SSM is a smoothing operation, rather than a deterministic static correction. Experience to date suggests that the method is most effective with near-surface irregularities which are of limited lateral extent and which are not adequately defined with traveltimes from intermediate shot-to-receiver distances. Furthermore, the GRM SSM appears to correct minor errors in picking traveltimes due to variations in signal-to-noise ratios.

As might be anticipated, near-surface irregularities also generate amplitude anomalies, in addition to time anomalies (Palmer, 2001c). A companion paper (Palmer, in prep.) describes an analogous process of correcting for the amplitude anomalies, using the geometric mean, in order to facilitate detailed inversion of the head wave amplitudes.

As with the GRM, the computations for the GRM SSM are simple arithmetic operations, which are readily implemented with any spreadsheet. Therefore, it is a relatively straightforward task to include both of these methods into any stream for the routine processing of shallow refraction data, in order to generate detailed starting models for further modelling with either tomographic methods or interactive manual methods of model-based inversion.

The application of the GRM and the GRM SSM can result is a significant improvement in the detailed lateral resolution of seismic velocities within the refractor. Equivalent resolution is not as easily achieved with model-based inversion methods, which employ simple algorithms to generate starting models.

REFERENCES

Ackermann, H.D., Pankratz, L.W., and Dansereau, D., 1986, Resolution of ambiguities of seismic traveltime curves: *Geophysics* **51**, 223–235.

Aki, K., and Richards, P.G., 2002, *Quantitative Seismology*: University Science Books.

Berry, M.J., 1971, Depth uncertainties from seismic first arrival studies: *Journal of Geophysical Research*, **76**, 6464–6468.

Dobrin M.B., 1976, *Introduction To Geophysical Prospecting*, 3rd edn: McGraw-Hill Inc.

Hagedoorn, J.G., 1955, Templates for fitting smooth velocity functions to seismic refraction and reflection data: *Geophysical Prospecting*, **3**, 325–338.

Hagedoorn, J.G., 1959, The plus-minus method of interpreting seismic refraction sections: *Geophysical Prospecting*, **7**, 158–182.

Hagiwara, T., and Omote, S., 1939, Land creep at Mt Tyausu-Yama (Determination of slip plane by seismic prospecting): *Tokyo University Earthquake Research Institute Bulletin*, **17**, 118–137.

Hawkins, L.V., 1961, The reciprocal method of routine shallow seismic refraction investigations: *Geophysics*, **26**, 806–819.

Healy, J.H., 1963, Crustal structure along the coast of California from seismic-refraction measurements: *Journal of Geophysical Research*, **68**, 5777–5787.

Lanz, E., Maurer, H., and Green, A.G., 1998, Refraction tomography over a buried waste disposal site: *Geophysics*, **63**, 1414–1433.

Leung, T.K., 1997, Evaluation of seismic refraction interpretation using first arrival ray tracing: in McCann, D.M., Eddleston, M., Fleming, P.J., and Reeves, G.M., (eds.), *Modern geophysics in engineering geology*: The Geological Society, pp391–398.

Leung, T.K., 2003, Controls of traveltime data and problems of the generalized reciprocal method: *Geophysics*, **68**, 1626–1632.

Nikrouz, R., Spyrou, A., and Palmer, D., Three dimensional (3D) three component (3C) shallow seismic refraction surveys across a shear zone associated with dryland salinity: in prep.

Oldenburg, D.W., 1984, An introduction to linear inverse theory: *Trans IEEE Geoscience and Remote Sensing*, **GE-22**, 666.

Palmer, D., 1980, *The Generalized Reciprocal Method Of Seismic Refraction Interpretation*: Society of Exploration Geophysicists.

Palmer, D., 1981, An introduction to the generalized reciprocal method of seismic refraction interpretation: *Geophysics*, **46**, 1508–1518.

Palmer, D., 1986, *Refraction Seismics: The Lateral Resolution of Structure and Seismic Velocity*: Geophysical Press.

Palmer, D., 1991, The resolution of narrow low-velocity zones with the generalized reciprocal method: *Geophysical Prospecting*, **39**, 1031–1060.

Palmer D., 1992, Is forward modeling as efficacious as minimum variance for refraction inversion?: *Exploration Geophysics*, **23**, 261–266, 521.

Palmer, D, 2001a, Imaging refractors with the convolution section: *Geophysics*, **66**, 1582–1589.

Palmer, D, 2001b, Resolving refractor ambiguities with amplitudes: *Geophysics*, **66**, 1590–1593.

Palmer, D, 2001c, Amplitude "statics" in shallow refraction seismology: *15th Geophysical Conference and Exhibition, Australian Society of Exploration Geophysicists*.

Palmer, D., 2003, Application of amplitudes in shallow seismic refraction inversion: *16th Geophysical Conference and Exhibition, Australian Society of Exploration Geophysicists*.

Palmer, D., Effects of near surface irregularities on refraction amplitudes, in prep.

Schuster, G.T., and Quintus-Bosz, A., 1993, Wavepath eikonal traveltime inversion: theory: *Geophysics*, **58**, 1314–1323.

Sjogren, B., 1984, *Shallow refraction seismics*: Chapman and Hall.

Slichter, L.B., 1932, Theory of the interpretation of seismic travel-time curves in horizontal structures: *Physics*, **3**, 273–295.

Stefani, J.P., 1995, Turning-ray tomography: *Geophysics*, **60**, 1917–1929

Treitel, S., and Lines, L., 1988, Geophysical examples of inversion (with a grain of salt): *The Leading Edge*, **7**, 32–35.

Whiteley, R.J., 2004, Shallow seismic refraction interpretation with visual interactive ray trace (VIRT) modeling: *Exploration Geophysics*, **35**, 116–123.

Zhang, J. and Toksoz, M.N. 1998, Nonlinear refraction traveltime tomography: *Geophysics*, **63**, 1726–1737.

Zhu, X., Sixta, D.P., and Andstman, B.G., 1992, Tomostatics: turning-ray tomography + static corrections: *The Leading Edge*, **11**, 15–23.

浅層屈折法データに対する静補正

D. パーマー[1]・R. ニクロウス[1]・A. スピロウ[2]

要　旨： 浅層屈折地震探査における屈折層の地震波速度の決定は、不良設定(ill posed)問題である。計算された時間パラメーターの小さな変化が、それらを用いて計算される速度に非常に大きな水平変化をもたらすことがある。それらは多くの場合、インバージョン・アルゴリズムに起因する偽像である。そのような偽像は、通常のモデル計算では認識されないし修正もされない。したがって、モデルに基づいた逆解析で詳細な屈折モデルを求めるような場合には、詳細な初期モデルが必要となる。地震波速度の偽像は不規則な屈折面形状に起因することが多い。ほとんどの状況下で、一般化相反屈折法(GRM)の可変マイグレーションは不規則な地層境界面に対応でき、屈折層の詳細な初期モデルを作成することができる。しかし、極浅層に不規則な構造が存在すると、GRM の効果は減少し、風化層補正が必要となる場合もある。

浅層不規則面の水平方向の連続性が限られている場合、通常の不規則面補正法は実用的ではない。そのような状況では、GRM のスムース静補正法(SSM)が簡易で間違いのないアプローチであり、それによって屈折層速度のより正確な評価を簡単に行うことができる。

GRM SSM では、種々の XY 値で計算された時間—深度対の平均をゼロ XY 値で計算された時間—深度対から引くことにより、平滑化した静補正値を生成する。より深い対象の時間—深度対は、XY 値が変化しても変化が小さいため、平均値と最適値はほぼ等しくなる。しかし、浅層屈折面での不規則な時間—深度対は、XY 値の増加に従って水平方向に移動し、それらはこの平均過程でかなり減少する。その結果、一連の XY 値について平均された時間—深度対は、浅層に不規則な屈折面が存在する場合にも有効に修正される。さらに、ゼロ XY 値で計算された時間—深度対は、浅層の効果と対象屈折面までの時間—深度対の両者の合計となる。したがって、逆にそれらの差は走時から差し引くための静補正の近似値となる。

GRM SSM は風化層を修正する決定論的アプローチというよりも、本質的には平滑化過程ということができる。この手法は水平方向に連続性が悪い、不規則な浅層屈折面に対して最も有効である。本論文では、不規則な屈折面の詳細な地震波速度決定の信頼性は GRM SSM を用いることにより大きく向上することを、モデル計算および事例研究によって示す。

천부 굴절법 탄성파 탐사 자료의 정보정

Palmer, D[1]・Nikrouz, R[1]・Spyrou, A[2]

요　약： 천부 탄성파 굴절법 탐사를 이용하여 굴절이 발생하는 지층의 속도를 산출하는 것은 ill-posed 문제이다. 계산된 시간 변수들에서의 작은 변화들이 이로부터 산출된 속도들에 커다란 수평적 변화를 가져올 수 있으며, 이는 종종 역산 알고리듬의 인위적인 오차를 유발한다. 이러한 인위적인 오차들은 모델링을 통해 인지되거나 보정되지 않는다. 그러므로 만약 모델에 근거한 역산을 통해 정밀한 지하 굴절 모델을 얻고자 한다면 정확한 초기 모델이 필요하다.

탄성파속도에서 인위적인 오차의 원인은 일반적으로 불규칙한 굴절면에 있다. 대부분의 경우에 GRM 방법을 이용하면 불규칙한 굴절면을 다룰 수 있고 굴절면의 정밀한 초기 모델을 만들 수 있다. 하지만 지표에 매우 가까운 극천부 지역 또한 불규칙하다면 GRM 방법의 효능은 감소하고 풍화대 보정이 필요하다.

천부 불균질대에 대한 일반적인 보정방법들은 수평적 확장이 제한된 극천부지역의 불균질대의 경우 효과적이지 못하다. 이럴 경우 GRM 평활화 통계적 방법(Smoothing Statics Method; SSM)이 지층의 속도를 좀 더 정확하게 평가할 수 있는 간단하고 실용적인 방법이다.

GRM SSM 방법은 제로 XY 값을 가지고 계산된 시간-심도값들로부터 실제 XY 값을 가지고 얻어진 시간-심도값들의 평균값을 빼줌으로써 평활화 정보정을 수행한다. 심도가 깊어질수록 시간-심도값들이 XY 값에 따라 크게 변하지 않으므로 이들의 평균값은 최적값과 훨씬 더 같아진다. 그러나 극천부의 불균질대에 대해 시간-심도값들은 XY 값들이 증가함에 따라 수평적으로 이동하고 평균화 과정을 통해 대폭 감소한다. 결과적으로, XY 값들에 대해 평균화된 시간-심도 단면도는 천부의 불균질대에 대한 보정에 효과적이다. 또한 제로 XY 값을 가지고 계산된 시간-심도값들은 천부 불균질대의 영향과 대상 굴절면에 대한 시간-심도값들의 합으로 주어지므로 그들의 차는 정보정을 위해 주시로부터 빼주어야 할 대략적인 값들을 제공한다,

GRM SSM 방법은 결정론적인 풍화대에 대한 보정법이라기 보다는 평활화 과정이다. 이 방법은 수평적으로 확장이 매우 제한된 천부 불균질대에 대해 가장 효과적이다. 모델과 현장 적용 결과들을 통해 GRM SSM 방법을 이용하여 불규칙한 굴절면을 가진 지층들에 대해 좀 더 신뢰할 수 있는 정밀한 탄성파 속도를 산출할 수 있음을 보여주고 있다.

1 School of Biological, Earth and Environmental Sciences, the University of New South Wales
Sydney, NSW 2052, Australia
2 School of Biological, Earth and Environmental Sciences, the University of New South Wales (Presently, Fugro Ground Geophysics Pty Ltd)

1 ニューサウスウエルズ大学 生物学・地球・環境学部
2 ニューサウスウエルズ大学 生物学・地球・環境学部（現在フグロ物理探査(株)）